CORNELL CBN 96-7

4 June 1996

Vibrating wire field-measuring technique *

Alexander Temnykh†

Laboratory of Nuclear Studies, Cornell University, Ithaca, NY 14853, USA

Abstract

The alignment of final focusing elements is very important issue for the particle accelerator performance. The technique described below is developed to provide this alignment for the CESR Phase III project. It is based on excitation of harmonics of wire vibration by lorentz forces between current in a wire and the local magnetic field. Experiments show high sensitivity of this technique and its convenience for application to the alignment of several elements placed along a wire as well.

1 Introduction

The presented work has been motivated by needs of the CESR Phase III upgrade. There are few specifications which were not met before. One of them is that superconducting quads must be placed inside detector with $4T$ of solenoidal magnetic field. It will result in the strong forces acting on the quads and causing quad displacements. So, the only one way to proper alignment is that the quads must be aligned in their final position with detector field on. Optical tools can not completely provide it because quads will be placed into cryostats and will not be available for observation. Another way to make alignment is the use of thin wire stretched along beam axis with an appropriated technique of field measuring.

*Work supported by the National Science Foundation

†On leave from BINP, Novosibirsk

There is a *Pulsed-Wire field measuring technique* developed by Warren and Elliot, see reference [1], and widely used now, see for example [2], [3]. It is based on the fact that when a pulse of current is passed through a wire it excites a transverse force proportional to the local transverse magnetic field. The force evolves into a wave on the wire that propagates to a sensor placed along the wire. By measuring wire motion versus time one can extract information about field distribution along wire. Unfortunately, there is difficulty with applying this method to the CESR upgrade project. The region what needs to be aligned is about 6 meters long. To avoid interference at the sensor location between waves carrying information about the magnetic field from inside region and waves reflected from wire's ends, the wire length must be at least twice as long as the measured region, i.e., 12 m long. It is not easy to arrange this space around the assembled interaction region for measurements. Another complication of this technique is the requirement of generating of high voltage short pulse needed for long wire.

The *Vibrating wire field-measuring technique* presented here will be more appropriated. It is based on the following. The stressed wire has fundamental mode of vibration with half wavelength equal to wire length and higher harmonics with shorter wavelength and higher frequencies. Suppose there is transverse magnetic field around wire. If the frequency of current in the wire is an eigenmode frequency, it will excite a corresponding harmonic. The strength of excitation will depend on the field distribution along the wire. Using various frequencies and measuring amplitudes and phases of resulting vibrations, one can extract information about the field distribution and reconstruct it. The field in turn shows the misalignment of magnetic elements.

In comparison with the pulsed-wire method, the vibrating wire technique does not require the wire length to be longer than the length of the test region, and due to extraordinary sensitivity it does not require higher voltage for long wire.

2 Theory

Figure 1 gives the scheme of setup used in experiments and in calculations below. A wire with tension T and length l has the fixed ends at $x = 0$ and $x = l$. The current in the wire, i.e., driving current, depends on time as $I(t) = I_0 exp(i\omega t)$. The wire crosses a region with horizontal magnetic field, $B_y(x)$, which is zero at the ends, $B_y(0) = B_y(l) = 0$. Consider vertical plane. There are two forces affecting the wire. They are gravity $g \cdot \mu$, where μ is mass of wire per unit of length, and the lorentz force $B_y(x) \cdot I(t)$.

The equation for vertical wire position, $U(x,t)$, will be:

$$\mu \frac{\partial^2 U}{\partial t^2} = T \frac{\partial^2 U}{\partial x^2} - \gamma \frac{\partial U}{\partial t} - \mu g + B_y(x) \cdot I_0 exp(i\omega t) \tag{1}$$

With bondary condition:

$$U(t,0) = U(t,l) = 0 \tag{2}$$

Here term $\gamma \frac{\partial U}{\partial t}$ describes damping. A general solution may be written in the form:

$$\begin{aligned} U(x,t) &= U_g(x) + U_d(x,t) \\ U_d(x,t) &= U_b(x) \cdot exp(i\omega t) \end{aligned} \tag{3}$$

Where $U_g(x)$ is the gravity term and $U_d(x,t)$ is the dynamic term caused by the interaction between the magnetic field and the driving current. An approximate expression for $U_g(x)$ is:

$$U_g(x) = -\frac{\mu g}{2T} x(x-l) \tag{4}$$

Note that at the point $x = l/2$ function $U_g(x)$ reaches its minimum which is the sag.

$$Sag = -\frac{\mu g}{8T} l^2 \tag{5}$$

Function $U_b(x)$, determined by magnetic field, may be found in the following way. As $U_b(x)$ satisfies the condition $U_b(0) = U_b(l) = 0$, it can be represented by fourier sine series:

$$U_b(x) = \sum_{n=1}^{\infty} U_n \sin\left(\frac{\pi n}{l} x\right) \tag{6}$$

Magnetic field $B_y(x)$, with similar boundary conditions, may be represented in the same way:

$$B_y(x) = \sum_{n=1}^{\infty} B_n \sin\left(\frac{\pi n}{l} x\right) \tag{7}$$

Substituting 3,4,6 and 7 into equation 1 we set:

$$\sum_{n=1}^{\infty} U_n \cdot \left(\omega^2 - \omega_n^2 + i\gamma\omega\right) \sin\left(\frac{\pi n}{l} x\right) = \sum_{n=1}^{\infty} \frac{I_0 B_n}{\mu} \sin\left(\frac{\pi n}{l} x\right) \tag{8}$$

where

$$\omega_n = 2\pi \frac{n}{2l} \sqrt{\frac{T}{\mu}} \tag{9}$$

Combining expression 9 with the formula for sag, (see 5), one can find a simple relation between sag and the fundamental mode frequency:

$$Sag = \frac{g}{32} \left(\frac{\omega_1}{2\pi}\right)^{-2} \tag{10}$$

It means that to obtain the sag we need only measure the fundamental frequency and using $g = 9.80665\, m/sec^2$ we can precisely calculate the sag.

By comparing the right and left sides of equation 8 one can find a connection between coefficients U_n and B_n:

$$U_n = \frac{I_0}{\mu\left(\omega^2 - \omega_n^2 + i\gamma\omega\right)} B_n \tag{11}$$

So, the time depended part of the general solution of equation 1 may be written as:

$$U_d(x,t) = \sum_{n=1}^{\infty} \frac{B_n \sin\left(\frac{\pi n}{l} x\right)}{(\omega^2 - \omega_n^2 + i\gamma\omega)} I_0 exp(i\omega t) \tag{12}$$

The following discussion conserns how we can obtain coefficients B_n of expansion 7 and reconstruct the magnetic field knowing the wire motion at the sensor location. Suppose the wire position sensor is located at the point $x = x_s$. Let us construct the function $\mathcal{F}(\omega)$ which is the time average of the product of wire position, $U_d(x_s, t)$, and driving current, $I(t)$:

$$\mathcal{F}(\omega) = \frac{1}{T} \int_0^T U_d(x_s,t) I(t) dt = \sum_{n=1}^{\infty} \mathcal{F}_n(\omega) \tag{13}$$

where:

$$\mathcal{F}_n(\omega) = \frac{B_n I_0^2}{2\mu} \sin\left(\frac{\pi n}{l} x_s\right) \frac{(\omega - \omega_n)}{4\omega(\omega - \omega_n)^2 + \omega\gamma^2} \tag{14}$$

Note that due to weak damping the wire motion has a high quality factor Q. It causes strong resonance amplification, and if the frequency of driving current is near ω_n, i.e., $\omega \approx \omega_n$, resonance term $\mathcal{F}_n$ in equation 13 will dominate over the rest. So we can write:

$$\mathcal{F}(\omega) \approx \mathcal{F}_n(\omega) \tag{15}$$

Suppouse we scanned the driving current frequency through one of resonance frequencies, ω_n. By recording both the driving current and signal from wire position sensor and doing numerical integartion, (see formula 13), we can measure function $\mathcal{F}_n(\omega)$. Then we must fit this mesurement with formula:

$$\mathcal{F}_n(\omega) = a_n \frac{(\omega - b_n)}{4\omega(\omega - b_n)^2 + \omega c_n^2} \tag{16}$$

where a_n, b_n, c_n are free parameters. Component B_n is obtained from a_n as:

$$B_n = a_n \frac{1}{\sin\left(\frac{\pi n}{l} x_s\right)} \frac{2\mu}{I_0^2} \tag{17}$$

Repeating this procedure for various ω_n, and using equation 7, we will reconstruct magnetic the field profile along the wire. Note that the resolution of reconstruction will depend on how many harmonics will be used and will be approximately equal to the shortest wavelength of the excited modes. Motion in horizontal plane does not differ from vertical except of gravity term.

The next section describes experimental application of the above theory.

3 Used equipment

Wire used in experiments was $100\,\mu m$ diameter made with alloy of copper-beryllium. As the type of wire was not critical, it was chosen to match what was mentioned in previous papers and was easy available.

LED-phototransistor assembly, (Motorola H21A1), was deployed as a wire position monitor. This kind of device was widely used in previous work, (see for example [2] and [4]). Figure 2 shows a schematic view of assembly with wire inside and electrical scheme around. The detector signal versus wire position is plotted on figure 3. There are two regions with linear dependence of signal on horizontal position with sensitivity about $1.8\,mV/\mu m$. The sensitivity to the vertical position is much less. It means that detector oriented as on figure 2 will see practically only horizontal wire motion and will not sensitive to vertical motion. To sense vertical motion detector must be rotated by 90 degree.

Macintosh Quadra 800 with Lab-NB Interface Board provided almost all needs of the measurements. An application program created in LabVIEW scanned the driving current frequency, recorded and manipulated signals, made fits and etc. Final output was the magnetic field measured along wire.

4 Measurement

A one meter long wire was used in the first modeling measurement. The wire motion detector was placed 7.5 cm from one of the ends. A small permanent magnet placed along wire created a magnetic field for testing. The strength of the field was controlled by the distance between magnet and wire.

Figure 4 and 5 illustrate the description given in the previous section. Plots in figure 4 show the results of excitation of the first five harmonics of 13 used in the measurement. Points show the measured function $\mathcal{F}(\omega)$ defined in the theoretical section and a line is fit to formula 15. There is good agreement between the measurement and fitting in all cases. The table on figure 4 shows parameters a_n obtained from fitting all 13 harmonics. Coefficients B_n calculated from a_n according to expresion 16 are in figure 5a. Field distribution reconstructed with formula 7 is plotted on figure 5b. It shows a very clear signal from the magnetic field. Note that the width of the signal $\sim 10\,cm$ is determined by the shortest wavelength used in the measurement harmonics. In this case the shortest wavelength was $8.65\,cm$ and was limited by the highest frequency the Lab-NB Interface Board was be able to generate.

Figure 6 shows the measured sensitivity of the vibrating-wire technique. To get the maximum of sensitivity the driving current amplitude was increased to its limit of $1\,A$. Other conditions were the same as in the previous measurements. The dashed line on figure 6 represents the measurement made without the test magnetic field, i.e., background. It shows the small negative magnetic field wich is equal to zero at the ends of wire. These zeros are due to specifics of measuring technique. Note that estimated value of the background field is less than $1\,gauss$. The dotted line shows the measurement when the small peace of permanent magnet was placed at the $5\,cm$ from wire to generate the test field. The result of subtraction of background from the latter represented by a solid line shows very clearly this field. The signal to noise ratio is less than $\pm 10\%$. Right scale and the line marked with points give the absolute value of the test field distribution along wire measured with Hall probe. It was $3.5\,gauss$ at the maximum, and approximately $5\,cm$ of length. Comparing wire and Hall probe measurements, one can see that the vibrating wire technique allows us to detect the location of less than $17.5\,gauss \cdot cm$ magnetic field errors. Note that for typical CESR's quads these errors correspond to less than $1\,\mu m$ misalignment!

Next experiments, suggested by David Rice, were to find the magnetic center of permanent magnet quad using a longer wire to simulate the condition of the interaction region alignment of the CESR Phase III upgrade project. Available setup space allowed a 3*meter* long wire. The test permanent magnet quad was $30\,cm$ long with a $14.8\,T/m$ gradient. Figures 7 and 8 show results of these experiments.

In the beginning the mechanical center of quad was adjusted to the wire position with traditional measuring tools, i.e., using rulers. The precision of this alignment was approximately $0.1\,mm$. Note that magnetic center of the quad may differ from its mechanical center.

Vibrating wire measurement gave horizontal field distribution shown by dotted line on figure 7. The square at the bottom shows the location and size of the test magnet. In the measurement 30 harmonics was used with shortest wavelength equal to $10\,cm$. It was 3 times shorter than the length of the test magnet and allowed us to see details of the field generated by magnet. Plot shows two unequal extremes of different polarities corresponding to the magnet ends. This kind of field distribution is due to a combination of tilt and shift of magnetic axes in the vertical plane relative to the wire. The solid line on figure 7 shows the final field distribution after a few iterations of measurement and adjustment of vertical quad position. It is approximately 10 times less than it was in the beginning.

By measuring the field difference produced by a known displacement of test quads, I calibrated measurements and estimated the residual misalignment seen on figure 7. Results are in figure 8. Here, the solid line shows the difference in field generated by a small vertical tilt of the magnet made with approximately $\pm 75\,\mu m$ magnet ends displacement. It caused $\pm 11.3\,gauss$ magnetic field change. One can see that the difference in the field looks like an antisymmetric function relative the middle of the magnet, as it should, with $\sim$ 2000 units amplitude. The dotted line is for a field difference due to $50\,\mu m$ vertical shift of magnet axis parallel to the wire. Here results a symmetric function with similar amplitude. So, referring to these measurements we can say that 1000 units corresponds to approximately $3\,gauss$ of magnetic field and estimate the residual misalignment seen on figure 7 as less than $50\mu m$. Note that this level of misalignment was determined by imperfect support of test magnets but not the measuring technique.

After the quad's magnetic center was adjusted to the wire position in vertical and in horizontal plane, using high precision optical instruments it was found that the misalignment between geometrical and magnetic center is in range between $125\,\mu m$ and $500\,\mu m$.

5 Conclusion

Vibrating wire technique developed and demonstrated above can provide adequate alignment of magnetic centers of final focusing quads for the CESR Phase III upgrade. Compared with the pulsed-wire technique, it looks more promising because it does not need space larger than the testing region and does not require generating very high voltage pulses on long wire with complicated measurement.

The wire sag must be taken into account for alignment. Its precise value may be obtained by measuring the frequency of fundamental mode of wire vibration, (see formula 10).

6 Acknowledgement

I thank James Welch, who motivated me to study the problem of magnet alignment. I am also very grateful to David Rice, David Rubin, Scott Chapman and Alexander Mikhailichenko for help.

References

[1] R. Warren and C. Elliot, *New System for Wiggler Fabrication and Testing*, Los Alamos National Laboratory, LA-UR 87-2981, (1987)

[2] R.W. Warren, NIM A272 (1988) 257-263

[3] C.M. Fortgang, et.al., *Pulsed Taut-Wire Alignment of Multiple Permanent Magnet Quadrupoles*, 1990 LINAC Conference, Albuquerque, NM, Sept. 1990.

[4] J.G. Melton, et.al., *Pulsed Taut-Wire Measurement of Magnetic Alignment of the ITS Induction Cells*, in Proceedings of the 1993 IEEE Particle Accelerator Conference, Catalog No. 0-7803-1203-1/9303.00, p. 2944

Figure 1: Scheme of vibrating wire experiments.

Figure 2: Schematic view of LED-phototransistor assembly used as a wire position detector.

Figure 3: Position monitor signal versus vertical and horizontal wire position.

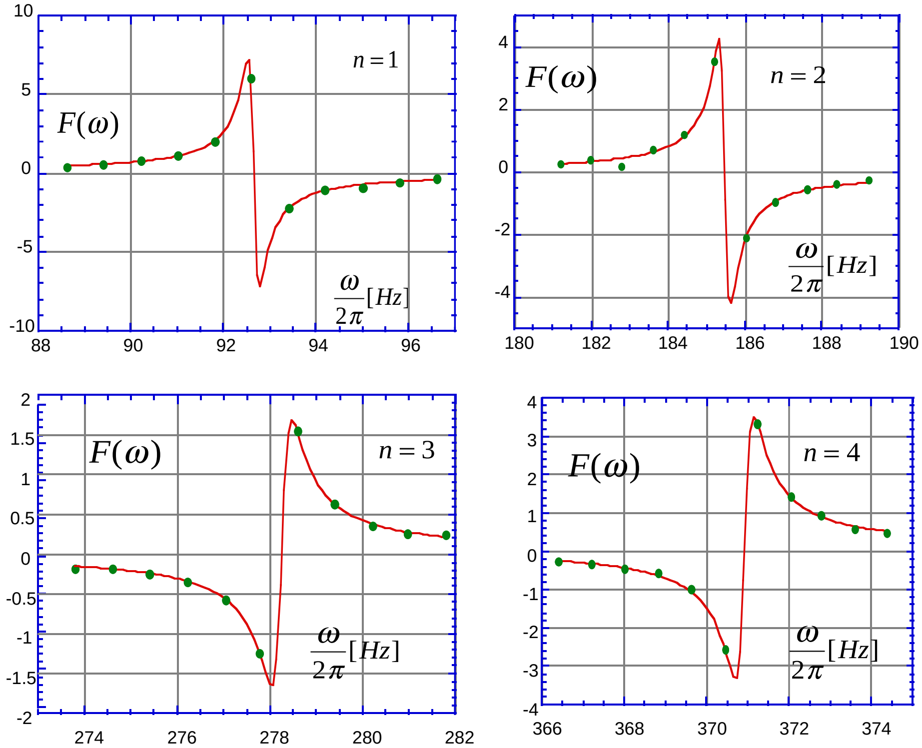

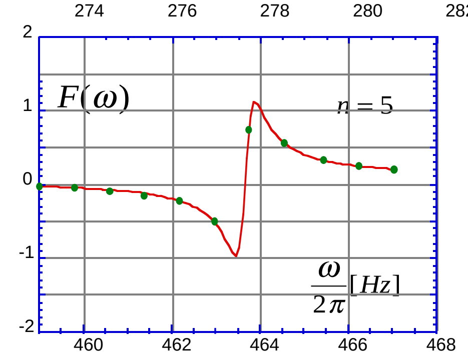

n	a(n)
1	6.76E+02
2	9.08E+02
3	-8.08E+02
4	-2.25E+03
5	-8.94E+02
6	1.82E+03
7	1.98E+03
8	-1.16E+02
9	-1.79E+03
10	-7.66E+02
11	4.83E+02
12	7.13E+02
13	7.62E+01

Figure 4: Measured function $\mathcal{F}(\omega)$ and coefficients a_n obtained from fitting. Points show measurements, lines are fits with formula $\mathcal{F}_n(\omega) = a_n \frac{(\omega - b_n)}{4\omega(\omega-b_n)^2 + \omega c_n^2}$

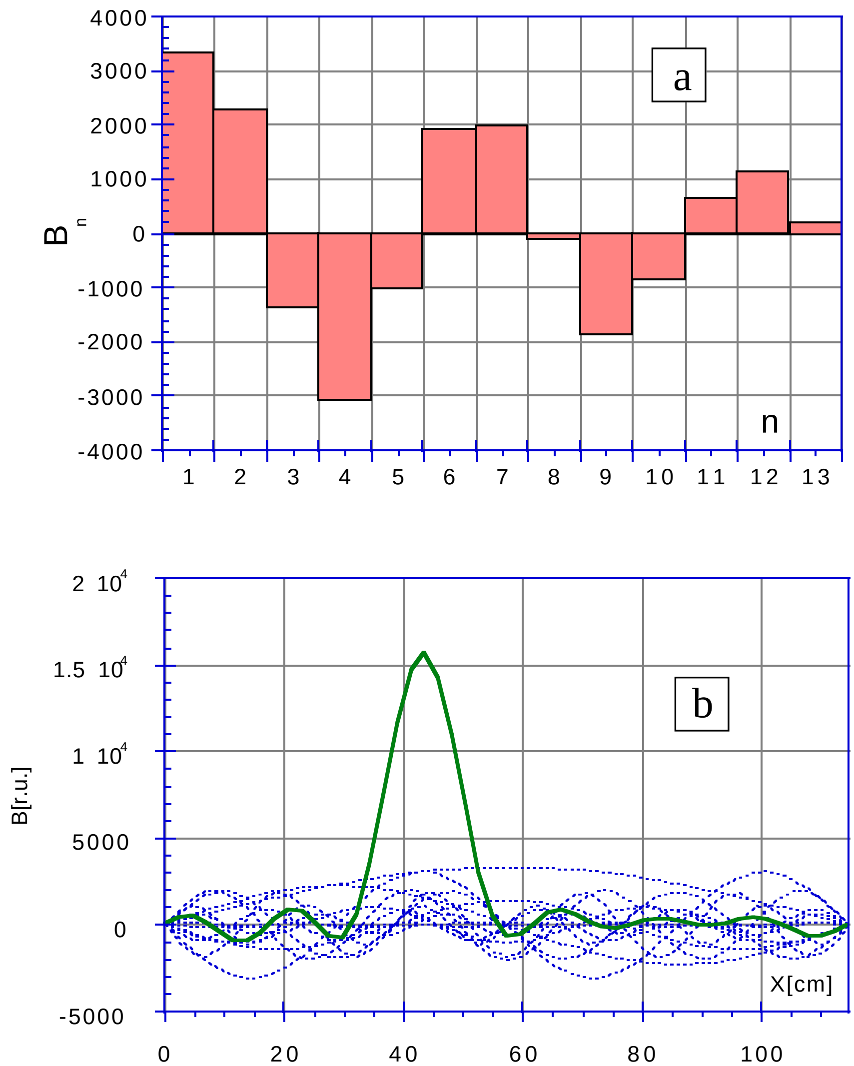

Figure 5: Components B_n, (see plot a), calculated from coefficients a_n and reconstructed magnetic field, (see plot b). Dotted lines show 13 harmonics corresponding to B_n.

Figure 6: Sensitivity of the vibrating-wire method. Dashed line shows background measurement. Dotted line is background plus test magnetic field. Solid line gives test field only. Right scale and line marked with points show Hall probe measurement.

Figure 7: Horizontal magnetic field along wire after conventional alignment, (see dotted line), and after vertical alignment with vibrating wire technique, (see solid line).

Figure 8: Dotted line shows the magnetic field difference caused by vertical $\pm 0.5\,mr$ tilt of testing quad. Solid line is the field difference due to vertical $50\,\mu m$ shift. Measurements were done using 30 harmonics with shortest wavelength of $10\,cm$.